

All-or-None Contraction and Sodium Channels in a Subset of Circular Muscle Fibers of Squid Mantle

WILLIAM F. GILLY¹, THOMAS PREUSS,¹ AND MATTHEW B. MCFARLANE²

¹*Departments of Biological Sciences and* ²*Molecular & Cellular Physiology, Hopkins Marine Station of Stanford University, Pacific Grove, California 93950*

Motor function in squid (Loligo) mantle reflects the highly coordinated activity of two motor pathways associated with giant and non-giant motor axons that respectively produce all-or-none and graded contractions in mantle muscle. Whereas both types of axons innervate circular mantle muscle fibers, precise nerve-muscle relationships remain unclear. Are squid like most invertebrates, in which single muscle fibers receive dual innervation from giant and non-giant motor axons, or is squid mantle configured more like vertebrates, in which parallel motor axon systems innervate distinct fast and slow muscle fibers? In this report, we describe giant and non-giant motor pathways that appear to control different pools of circular muscle fibers in squid. A subset of circular muscle fibers possesses large Na currents, and these fibers are proposed to employ Na-dependent action potentials to produce fast, all-or-none muscle twitches associated with giant axon stimulation.

Fast and slow motor systems with diverse properties occur in many taxa (1). Studies on arthropods and chordates have revealed remarkable differences in basic neuromuscular organization, but comparative knowledge of other groups is relatively limited. Dual motor pathways also exist in cephalopod molluscs (2). In many squid species, giant motor axons innervate extensive mantle fields composed of small-diameter, circular muscle fibers, and a single axonal impulse generates a powerful all-or-none twitch (3). A parallel set of non-giant motor axons acts to generate graded mantle contractions with repetitive stimulation (4, 5). Concerted recruitment of these two systems plays an important role in controlling jet-pro-

duced escape responses (6). Cephalopod muscle fibers are very small, and patterns of innervation for the two motor systems have not been elucidated.

Relative contributions to the mantle twitch made by these two motor pathways in squid can be evaluated by measuring contractile force due to circular muscle fibers in response to selective stimulation of giant and non-giant motor axons. In Figure 1A, a single shock excited only non-giant axons, and a stronger shock exceeded threshold for giant axon stimulation (Fig. 1B). Repetitive non-giant activity was stimulated by a brief, weak tetanus, and the resulting contractile response (Fig. 1C) is directly compared to the giant-driven response in Figure 1D (trace C versus B). The algebraic sum of traces B and C (B + C, dotted trace) is smaller than the response generated by a burst of strong shocks that excited both systems (thick trace) but is quite similar in time course. Thus, outputs of the two motor systems are roughly additive and combine to produce a powerful mantle contraction with a fast rise time.

Analysis of the relevant circular muscle elements has been limited, however. Three concentric layers of circular muscle fibers exist in squid mantle, with two superficial layers of mitochondria-rich fibers surrounding a much thicker central zone of smaller diameter, glycolytic fibers (7, 8). Based on these findings, it is believed that the central zone, innervated by the giant axons, generates escape jetting and that the superficial layers control slower, sustained swimming (2). Several observations, however, suggest that this division of labor is too simple. First, the superficial layers constitute no more than 20% (7, 8) of the total circular muscle mass, and it therefore seems unlikely that this small fraction could generate a twitch as large as that produced by stimulation of the giant axon (Fig. 1). Second, behavioral experiments indicate that squid can swim at variable velocities up to

Received 7 August 1996; accepted 21 August 1996.

Abbreviations: G_{Na} , Na conductance density; GFL, giant fiber lobe; I_K , K current; I_{Na} , Na current.

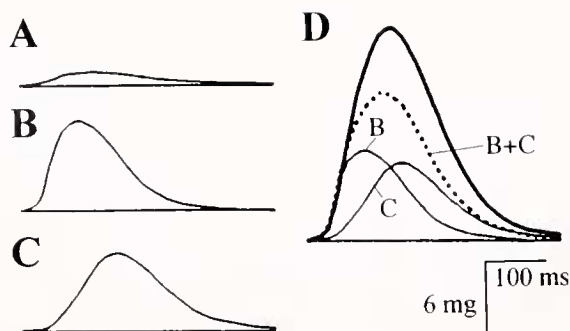


Figure 1. Non-giant and giant motor axons contribute approximately equally and additively to the twitch of circular muscle fibers. The nerve-muscle preparation consisted of a stellate ganglion from a juvenile *Loligo opalescens* connected by stellar nerves to a sector of mantle cut parallel to the circular muscle bands and attached to a force transducer (BG-10GM, Kulite Inc., Leonia, NJ). Motor axon stimulation was effected with a coaxial, bipolar electrode. (A) A single 3 V shock excited only non-giant motor axons. (B) A single 5 V shock exceeded threshold for giant axon excitation. (C) Summed response due to stimulation of non-giant motor axons with five 3 V shocks at 50 Hz. (D) Superposition of the records in panels B and C along with their algebraic summation (B + C, dotted trace) is compared with the responses to five 5 V shocks at 50 Hz which excite giant and non-giant motor systems. External solution was artificial seawater. $T = 16^{\circ}\text{C}$.

and including those characteristic of escape jetting (9). Third, giant and non-giant axon-driven responses can contribute nearly equally to escape jetting (6).

As a first step towards definition of the relevant neuromuscular relationships in squid muscle, we have attempted to identify a muscle fiber type with electrical properties suggestive of all-or-none excitability, and which therefore is likely to be associated with the giant axon system. Whole-cell voltage clamp recordings from dissociated mantle muscle fibers were carried out using a Na-containing internal solution that blocks K channels (10). Figure 2A illustrates a muscle fiber shortly after achieving the whole-cell configuration and after repetitive pulsing (inset), which caused irreversible contraction. This phenomenon reliably yielded well-clamped cells, and all data in this paper were similarly obtained. Transient inward current recorded from this muscle fiber at 0 mV (Fig. 2B_i) is eliminated by an inactivating prepulse (+pre; 50 ms to -30 mV) or by tetrodotoxin (+TTX; 500 nM). Figure 2B_{ii} illustrates analogous records from a cultured giant fiber lobe (GFL) neuron in which Na currents (I_{Na}) have been studied in detail (10). A family of prepulse-sensitive current traces from this muscle fiber (Fig. 2C) indicates a reversal potential close to the expected Nernst potential for Na ($\sim +20$ mV).

Taken together, these features demonstrate that this muscle fiber displays I_{Na} much like that in GFL neurons or the giant axon. This is not true for all mantle muscle fibers, however. Current records at 0 mV are illustrated

for three different muscle cells in Figures 3A–C. These recordings were made with a high K internal solution (11) in order to assay both inward I_{Na} and outward K currents (I_{K}). Long fibers of very thin diameter (Fig. 3A) exhibited robust I_{Na} , whereas larger diameter fibers (Fig. 3B) typically showed no or very little I_{Na} . Regardless of the I_{Na} level, all fibers expressed substantial I_{K} . Multipolar muscle cells (Fig. 3C) were also regularly encountered, and these too showed no I_{Na} . With the internal solution designed to eliminate I_{K} , all cell types displayed small, non-inactivating inward currents with properties similar to Ca currents in GFL neurons (12).

To more accurately compare Na channel density in different muscle cells, maximum Na conductance for each cell was computed from the final slope of the peak

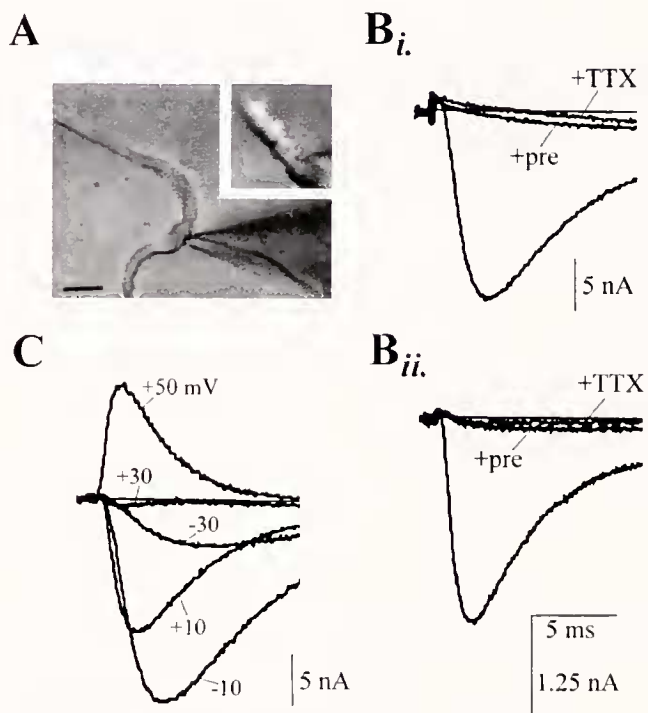


Figure 2. I_{Na} in a muscle fiber from squid mantle. Skinned mantles from juvenile squid (55–57 days old) were cut into strips parallel to circular muscle bands in Ca-free seawater and treated with protease (Type XIV, Sigma) for 40 min at 17°C . Strips were triturated through a micropipette to dissociate muscle fibers, which were then maintained up to one day at 17°C in a low-Ca medium (adapted from (15), external Ca = 2–3 mM). (A) Video prints during a whole-cell recording (see text for details; scale bar for this and all video prints = 20 μm). (B_i) Inward current at 0 mV (holding potential = -80 mV for this and all other figures) from the fiber in panel A without (large amplitude trace) and with either a depolarizing prepulse (+pre) or exposure to 500 nM tetrodotoxin (+TTX) in the external solution. (B_{ii}) Records obtained in a GFL neuron (6 days in culture) using the same apparatus and under identical conditions as used for panel B_i. (C) A family of I_{Na} currents (obtained by subtraction of records taken with and without an inactivating prepulse) recorded at the indicated voltages from the muscle fiber of panel A. External solution was culture medium. $T = 10 - 12^{\circ}\text{C}$.

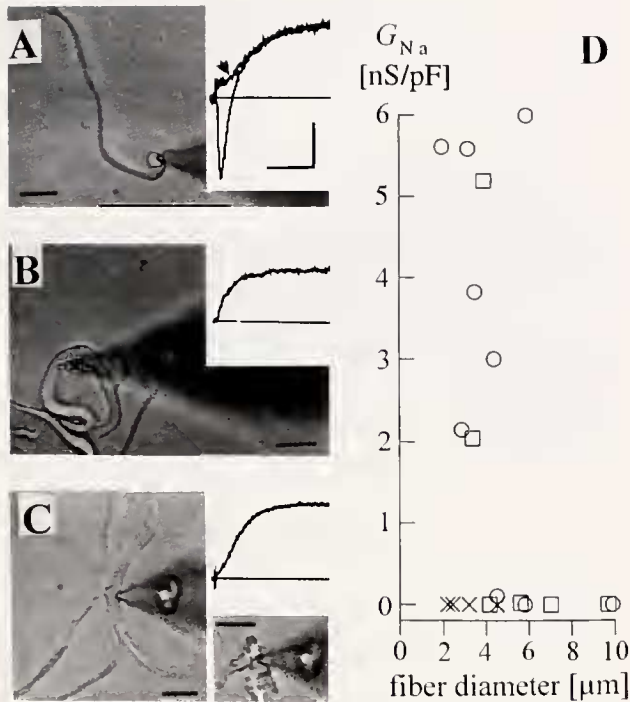


Figure 3. Correlation of Na channel expression and muscle fiber type. All data were derived as in Fig. 2. (A–C) Video prints of three different muscle cells taken shortly after achieving the whole-cell configuration and records of membrane current at 0 mV attained after contracture (inset in Fig. 3C). Currents in Fig. 3A are shown with and without a prepulse to inactivate I_{Na} . I_{Na} was not detectable in the fibers shown in panels B or C (for all current traces, vertical scalebar = 125 pA/pF, horizontal scalebar = 5 ms). (D) Specific Na conductance (G_{Na} ; derived as described in text) is shown plotted versus muscle cell diameter and type (see text for details). Diameter measurements were made from digitized video frames using image analysis software (NIH-Image 1.60), and mean diameter was calculated from 10 measurements equally spaced along the length of the fiber.

$I_{\text{Na}} - V$ relation, and these values were normalized by input capacity (G_{Na} ; nS/pF). These data are plotted versus diameter in Fig. 3D for fibers $< 120 \mu\text{m}$ (\square) and $> 120 \mu\text{m}$ (\circ) in length, and for multipolar-cell arms (\times). The approximate thickness of the mantle musculature is $120 \mu\text{m}$ (equal to the length of radial muscle fibers) in a squid of the size used for the dissociations (unpub. data). Fibers longer than this value are thus likely to be derived from circular muscle. Seven out of eight fibers showing significant G_{Na} lie in the 2–5 μm range, and most of these are $> 120 \mu\text{m}$ long. All fibers lacking G_{Na} are $> 4 \mu\text{m}$ diameter, and half of these are $> 120 \mu\text{m}$ long.

Thus, on the basis of the level of G_{Na} , we conclude that two classes of circular muscle fibers exist, and there appear to be two corresponding size classes. Presumably the small, Na-channel-rich fibers are central circular fibers ($3.3 \pm 0.1 \mu\text{m}$ diameter, mean \pm SEM based on unpublished electron microscopic analysis) associated with

the giant axon system, but at present we have no direct evidence. Identification of long fibers devoid of Na channels is less certain. These fibers could either be superficial fibers ($4.8 \pm 0.2 \mu\text{m}$ diameter), or they could represent a distinct type of central fiber associated with the non-giant motor system that contributes to escape jetting. Although anatomical studies have not revealed two types of central circular fibers, existence of a central fiber type showing graded excitability is suggested by the relatively large contribution conferred by repetitive stimulation of non-giant motor axons (Fig. 1C).

Multipolar cells also appear to lack Na-channel-based excitability. This unusual cell type has not been previously detected in anatomical studies, but the small diameter and overall length of the processes would be consistent with the idea that such cells represent radial muscle fibers ($2.7 \pm 0.2 \mu\text{m}$ diameter). Future studies will be required to test this hypothesis. Graded excitability in this type of muscle fiber would fit with the role played by radial fibers *in vivo* (13).

Results in this paper demonstrate the existence of large Na currents in circular muscle fibers of squid mantle, and we propose that these currents provide the basis for the all-or-none contractile response to a single action potential in the giant motor axons. Na-channel-based excitability in invertebrate muscle fibers was previously reported to exist only in the phylum *Chaetognatha* (comprising the “arrow worms”, ref. 14). Theories concerning the evolutionary origin of Na channels in muscle fibers of deuterostome versus protostome invertebrates must also take the data on squid described in this study into account. Clearly, application of patch-voltage clamp techniques to muscle fibers from a wide variety of invertebrate phyla would be a valuable contribution to comparative muscle physiology and might provide insights of evolutionary significance.

Acknowledgment

This work was supported by grants from the National Institutes of Health, the National Science Foundation, the Office of Naval Research, and the Ford Foundation. We are grateful to Gilbert van Dykhuizen (Monterey Bay Aquarium) for providing juvenile squid.

Literature Cited

1. Hoyle, G. 1983. *Muscles and Their Neural Control*. Wiley, New York.
2. Bone, Q., E. R. Brown, and M. Usher. 1995. The structure and physiology of cephalopod muscle fibres. Pp. 301–309 in *Cephalopod Neurobiology*; N. J. Abbot, R. Williamson, and L. Maddock eds. Oxford University Press, New York.

3. Young, J. Z. 1938. The functioning of the giant nerve fibres of the squid. *J. Exp. Biol.* **15**: 170-85.
4. Prosser, C. L., and J. Z. Young. 1937. Responses of muscles of the squid to repetitive stimulation of the giant nerve fibres. *Biol. Bull.* **73**: 237-41.
5. Wilson, D. M. 1960. The control of movement in cephalopods. *J. Exp. Biol.* **37**: 57-72.
6. Otis, T. S., and W. F. Gilly. 1990. Jet-propelled escape in the squid *Loligo opalescens*: concerted control by giant and non-giant motor axon pathways. *Proc. Natl. Acad. Sci. USA* **87**: 2911-5.
7. Bone, Q., A. Pullsford, and A. D. Chubb. 1981. Squid mantle muscle. *J. Mar. Biol. Assoc. UK* **61**: 321-42.
8. Mommsen, T. P., J. Ballantyne, D. MacDonald, J. Gosline, and P. W. Hochachka. 1981. Analogues of red and white muscle in squid mantle. *Proc. Natl. Acad. Sci. USA* **78**: 3274-8.
9. O'Dor, R. K. 1988. The forces acting on swimming squid. *J. Exp. Biol.* **137**: 421-42.
10. Gilly, W. F., and Brismar, T. 1989. Properties of appropriately and inappropriately expressed sodium channels in squid giant axon and its somata. *J. Neurosci.* **9**: 1362-74.
11. Gallant, P. E. 1988. Effects of the external ions and metabolic poisoning on the constriction of the squid giant axon after axotomy. *J. Neurosci.* **8**: 1479-84.
12. McFarlane, M. B., and W. F. Gilly. 1996. Spatial localization of calcium channels in giant fiber lobe neurons of the squid (*Loligo opalescens*). *Proc. Natl. Acad. Sci. USA* **93**: 5067-71.
13. Gosline, J. M., J. D. Sleeves, A. D. Hartman, and M. D. Demont. 1983. Patterns of circular and radial muscle activation in respiration and jetting of the squid, *Loligo opalescens*. *J. Exp. Biol.* **104**: 97-109.
14. Schwartz, L., and W. Stuhmer. 1984. Voltage-dependent sodium channels in an invertebrate striated muscle. *Science* **225**: 532-5.
15. Gilly, W. F., M. T. Lucero, and F. T. Horrigan. 1990. Control of the spatial distribution of sodium channels in giant fiber lobe neurons of the squid. *Neuron* **5**: 663-674.